Advances in Bioresearch
Adv. Biores., Vol 12 (2) March 2021: 01-12

Print ISSN 0976-4585; Online ISSN 2277-1573
Journal's URL:http://www.soeagra.com/abr.html
CODEN: ABRDC3
DOI: 10.15515/abr.0976-4585.12.2.112

Advances in Bioresearch

ORIGINAL ARTICLE

A Study on Degradation of Methyl Orange under UV Light Irradiation and Ammonia Gas Sensing by Polypyrrole/ Lead Selenide Nanocomposite

Manoharmayum Vishwanath Sharma[1], Harendra Kumar Sharma[1]* and Nimisha Jadon[2]
[1]School of Studies in Environmental Science (IGAEERE), Jiwaji University, India
[2]School of Studies in Environmental Chemistry, Jiwaji University, India
Email: drsharmahk@yahoo.com

ABSTRACT
Lead selenide nanomaterial was synthesized using co-precipitation method and polymerization of pyrrole was done in the presence of the synthesized lead selenide nanomaterial to prepare ppy/lead selenide nanocomposite. The synthesized materials were characterized using TEM, SAED, XRD, FTIR, UV-Vis Spectroscopy. The synthesized lead selenide nanomaterial was found to less than 10 nm in size and crystalline in nature with crystallite size of 4.83 nm. The TEM showed that the lead selenide nanomaterial is embedded in the ppy matrix. The FTIR analysis indicated presence of peaks only in the fingerprint reason of the IR spectra. The synthesized ppy/lead selenide nanocomposite was found to be able to degrade methyl orange up to 83.13 % under optimized condition of Irradiation time with UV light, dose of nanomaterial, concentration of dye and pH of the dye solution and showed a sensitivity of 57.78 % at 10 ppm of ammonia gas. The study indicated that the photocatalytic potential of ppy/lead selenide nanocomposite is viable material for application in methyl orange degradation and for ammonia gas sensing.
Keywords: Polypyrrole, Lead selenide, Nanocomposite, Photocatalysis, Gas Sensing.

Received 24.10.2020 Revised 22.11.2020 Accepted 27.01.2021

How to cite this article:
M V Sharma, H K Sharma and N Jadon. A Study on Degradation of Methyl Orange under UV Light Irradiation and Ammonia Gas Sensing by Polypyrrole/ Lead Selenide Nanocomposite. Adv. Biores. Vol 12 [2] March 2021. 01-12

INTRODUCTION

Nanomaterials have been documented to have a broad range of applications in different fields [1,2]. Due to their promising physical, optical properties and gas sensing properties, polymer composites have become more and more relevant. Different researchers have investigated the synthesis of various chalcogenides [3–5]. The electroluminescence and various diffractive properties of nanocomposites of chalcogenide/polymer have recently been investigated [6–8]. For its use in optoelectronics, photosynthetic and photocatalytic applications, metal selenides have been synthesized. The properties of both, resulting in a multifunctional material, can be inherited by composites synthesized combining chalcogenide and organic polymer. Organic polymers have strong photoinduced effects and poor stability, while chalcogenides have low photoinduced effects and excellent stability [9]. Methyl orange dye is extremely toxic and may be lethal if inhaled, ingested or absorbed into the skin. A delayed impact of touch or inhalation can be seen. Methyl orange upon fire can also generate irritating, corrosive and/or harmful gases and may be corrosive and/or toxic and cause contamination by runoff from fire suppression or water dilution [10].Ammonia with a threshold limit of 25 ppm, a short-term exposure limit of 35 ppm belongs to a category of toxic gases that, if exposed, damage the respiratory systems, eyes and skin. Ammonia hydrolysis contributes to the formation of ammonium hydroxide that can cause upper respiratory tract and eye irritation, as ammonium hydroxide is a strong base [11]. It also plays a role in the formation of harmful PM 2.5 secondary fine particulates[12].

Understanding the problem that these two substances present the current research focuses on photocatalysis of methyl orange dye and ammonia gas sensing by using polypyrrole (ppy)/lead selenide nanocomposite.

MATERIAL AND METHODS

Experimental Section

Analytical grade chemicals and reagents used in the experiment as received without any purification.

Synthesis of Metal Lead Selenide Nanomaterial

In a beaker, Ethylene glycol, hydrazine hydrate and double distilled water with a ratio of 3:1:7 were taken and mixed with a magnetic stirrer for 30 minutes. 1 g of lead chloride salt was then added and stirred for another 30 minutes to facilitate the dissolution. 0.5 g of selenium powder was added to his solution and refluxed for 6 hat 60^0 C. the dark precipitate that formed was collected using vacuum filtration and washed for 5 times with ethanol and double distilled water. Using the vacuum pump, the dark residue was air dried for 20 minutes and then dried for 48 hours at 60^0 C in the a hot air oven [13]. The dried sample was then suvbsequently used for the used for preparation of polypyrrole (ppy)/lead selenide nanocomposite.

Synthesis of Polypyrrole/LeadSelenide Nanocomposite

30% of synthesized lead selenide nanomaterial by weight of pyrrole was added into 1 M solution of pyrrole was taken in a beaker and ultrasonicated for 30 mins. 1 M solution of Ferric chloride solution was then added drop by drop using a dropping funnel into the 1 M pyrrole solution under constant stirring with a magnetic stirrer. In order to permit complete polymerization of pyrrole a ratio of 1:2.4 was maintained between pyrrole and ferric chloride. The solution mixture was maintained at 5^0 C by using an ice bath and thermometer. The colour of the solution resulted in a dark precipitate with a greenish hue, showing that the pyrrole was polymerized into polypyrrole(ppy). This solution mixture was left for 24 hours to allow complete polymerization and the residue was separated by means of a vacuum filtration. The separated dark greenish residue was washed with absolute ethanol and double distilled water 5 times. It was air dried for 20 min then in a hot air oven for 48 h at 60 º C[14]. The dried powder sample was characterized and utilized for the photocatalysis of methyl orange and ammonia gas sensing study.

Characterization

The synthesized ppy/lead nanocomposite was characterized at Jiwaji University, India's Central Instrumentation Facility. The specifications of the instruments for characterization are **Powder X-Ray Diffraction (Rigaku- Modal no Mini Flex 600), Fourier Transformation Infrared** Spectroscopy (**Perkin Elmer Modal no. Spectrum Two Serial no. 105627 FT-IR), Transmission Electron Microscopy (**JEOL 1230) and UV-Visible Spectroscopy (Shimadzu UV-1280 Multipurpose UV-Visible Spectrophotometer).

Photocatalytic Degradation of Methyl Orange

Methyl orange was used to explore the photocatalytic potential of the synthesized ppy/lead selenide nanocomposite. Experimental parameters such as uv light effects of irradiation, dose effects, concentration and pH effects on methyl orange dye degradation have been studied. The 365 nm and 254 nm (6 Watt) UV lamps were used at the same time to irradiate the dye solution. a distance of 15 cm from the uv lamp was maintained for all samples.

Gas Sensing Measurement

Drop-cast method was used to deposit thin films of ppy/lead selenide nanocomposite over the glass slide (20 mm x 20 mm) and dried at 45º C. Using a copper electrode for contact LCR meter (Hioki 3232) was used for the electrical measurement. The sensor activity was investigated by a simple net-volume gas chamber 10 cm x 10 cm x 10 cm. The chamber was fed with 2 ppm, 4 ppm, 6 ppm, 8 ppm, and 10 ppm ammonia gas levels. The moisture in the room was 40% and the temperature was 25-30^0 C. The sensitivity (response) percentage of the sensor was calculated by [15]

$$S\ (Response) = \frac{\Delta R}{R_g}\ X\ 100 \qquad (i)$$

where ΔR is the change in resistance, and $R_g$is the resistance upon exposure to ammonia gas.

Results and Discussions

Transmission Electron Microscopy (TEM)

The TEM ananlysis showed that the synthesized lead selenide nanomaterials are of homogenous form and dimension (Fig. 1a). It is less than 10 nm in size range. The nanomaterial for lead sulphide can also be seen integrated in the ppymatrixalong with some minor agglomeration (Fig. 1b).

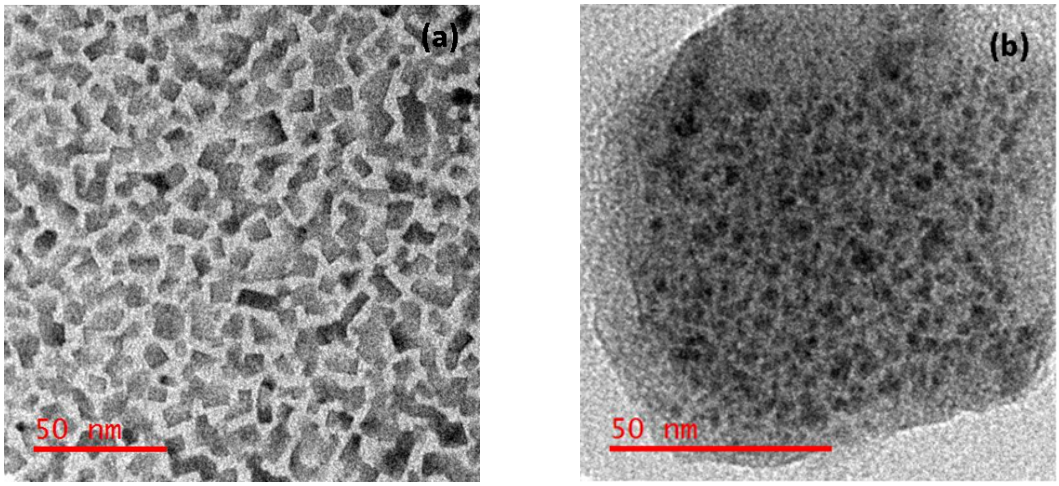

Fig. 1. TEM micrograph of (a) lead selenide and (b) ppy/ lead selenide nanocomposite

Selected Area Electron Diffraction (SAED)

The analysis of SAED (Fig. 2) showed a polycrystalline lead selenide nanomaterial. The crystalline nature of the lead selenide nanomaterial is evident from the presence of discreet rings in the SAED pattern. The SAED pattern of ppy/lead selenide nanocomposite shows the presence of a lower- intensity spot, which indicates both crystalline and amorphous material characteristics.

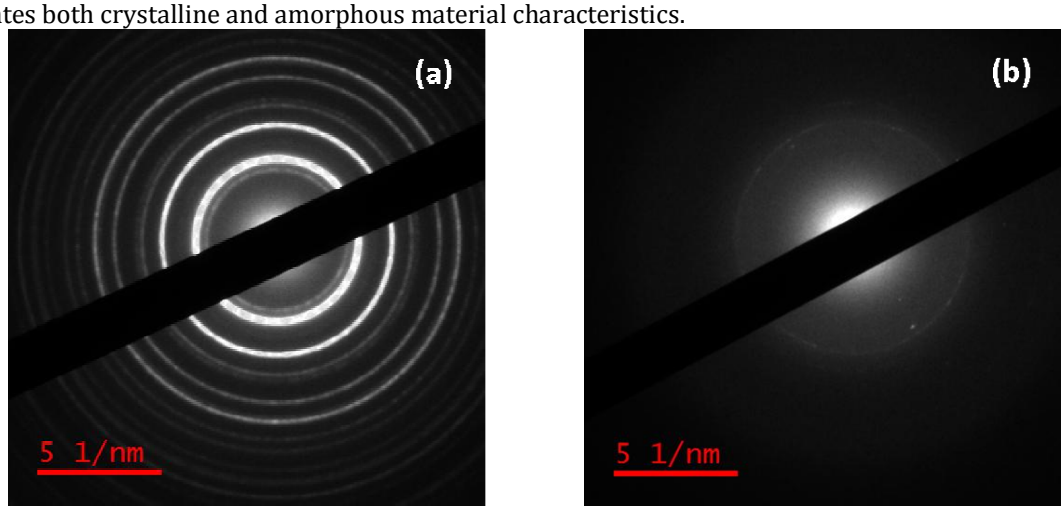

Fig 2. SAED pattern of (a) lead selenide and ppy/lead selenide nanocomposite

X-Ray Diffraction Analysis (XRD)

In lead selenide nanomaterials, the powder XRD analysis also shows sharp peaks, indicating that the nanomaterial is crystalline. For ppy/lead selenides, the presence of sharp peaks with a wide base shows crystalline and amorphous material characteristics, as large peaks and sharp peaking indicate amorphous and crystalline materials respectively.

The synthesized lead selenide nanomaterial's crystallite size was calculated with the Scherrer formula [16] from the XRD spectra and it was found to be 4.83 nm.

$$\textit{Scherrer's formula, } \tau = \frac{K\lambda}{\beta Cos\theta} \qquad \textit{(ii)}$$

Where τ is the crystallite size, K is a crystallite shape factor, λ is the wavelength of X-ray, β is the full width at half maximum of the X-ray diffraction peak and θ is the Bragg angle.

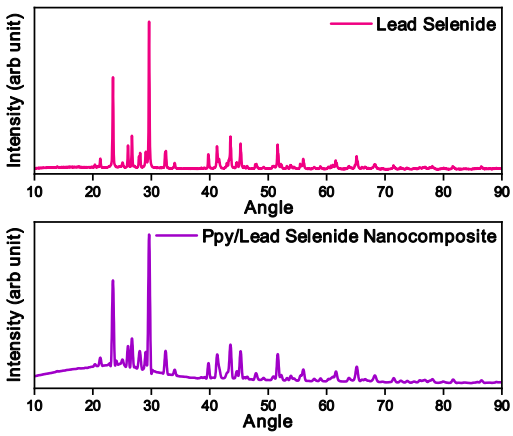

Fig. 3. XRD spectra of lead selenide and ppy/ lead selenide nanocomposite

Fourier Transformation Infra-Red Spectroscopy (FTIR)

The FTIR study of the synthesized lead selenide nanomaterial showed peaks in the fingerprint region of the IR spectra in the both lead selenide nanomaterial and ppy/lead selenide nanomaterial (Fig. 3). Lead selenide nanomaterial shows peaks at 1371 cm^{-1} and655 cm^{-1} for indicating the presence of the functional groups CH_2/CH_3 and C-H respectively which are due to the presence of residue from ethanol washing but in the case of ppy/lead slenide nanomaterial several peaks are shown. Apart from these functional groups there are no significant presence any functional group in the synthesized lead selenide nanomaterials. The peaks positions and their respective functional groups for ppy/lead selenide nanocomposite have been given in Table 1.

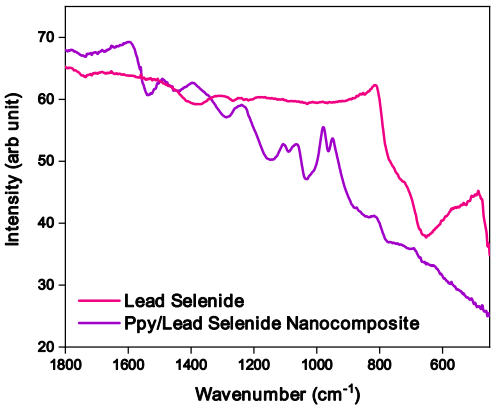

Fig 4. FTIR analysis of lead selenide and ppy/ lead selenide nanocomposite

Table 1. Fuctional Groups as shown by FTIR study of ppy/ lead selenide nanocomposite

Peak Position (cm^{-1})	Funtional Groups
1536	NH out of plane
1436	C-C stretch
1289	C-H wag
1148	C-N stretch
1089	C-N stretch
1031	C-N stretch
846	C-H out of plane
780	C-H out of plane
664	C-H bend

Uv-Visible Spectroscopy

The UV-Spectroscopy analysis of the synthesized lead selenide and ppy/lead selenide nanomaterial (Fig. 5) indicated that the highest absorbance of the nanocomposite was at 578 nm and 346 nm respectively.

The band gap energy was calculated using the Energy Equation of Quantum Mechanics [17] which is given by

$$E_g = \frac{hc}{\lambda_g} \qquad (iii)$$

Where E_g is the band gap energy, h is the Plank's constant, c is the velocity of light and λ_g is the wavelength of maximum absorbance. The bandgap energy of the synthesized lead selenide nanomaterial and ppy/lead selenide nanocomposite were calculated to be 2.15 eV and 3.58 eV respectively.

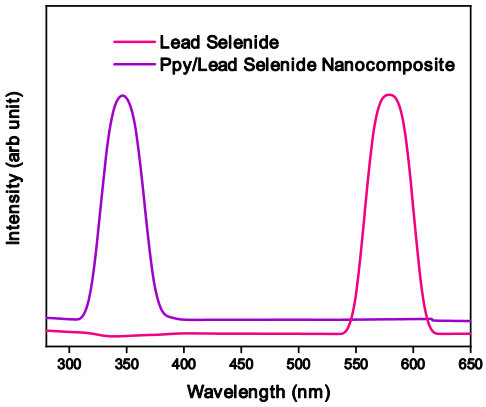

Fig. 5. UV-Vis Spectra of lead selenide and ppy/ lead sulphide nanocomposite

Dye Degradation

The formation of radicals in the process of photoexcitation of semiconductor photocatalyst has been reported to be responsible for the degradation of the dyes.The dye degradation potential was calculated using the formula [18]:

$$Degradation\ (\%) = \frac{C_i - C_f}{C_i} \times 100 \qquad (iv)$$

Where C_i is the initial concentration and C_f is the final Concentration of Methyl Orange Dye. The below given reaction and mechanism (Fig. 6) can be considered for the degradation of methyl orange [19].

Photocatalyst + hν (Photons) → e^- (CB) + h^+ (VB)

$h^+ + H_2O \rightarrow H^+ + OH^-$

$h^+ + OH^- \rightarrow OH\bullet$

$e^- + O_2 \rightarrow O_2\bullet$

$2e^- + O_2 + H_2O \rightarrow H_2O_2$

$e^- + H_2O_2 \rightarrow OH\bullet + OH^-$

Methyl Orange + $OH\bullet + O_2 \rightarrow CO2 + H_2O$ + Other products from degradation

(e^-= electron, h^+= electron hole, CB= Conduction Band, VB= Valence Band)

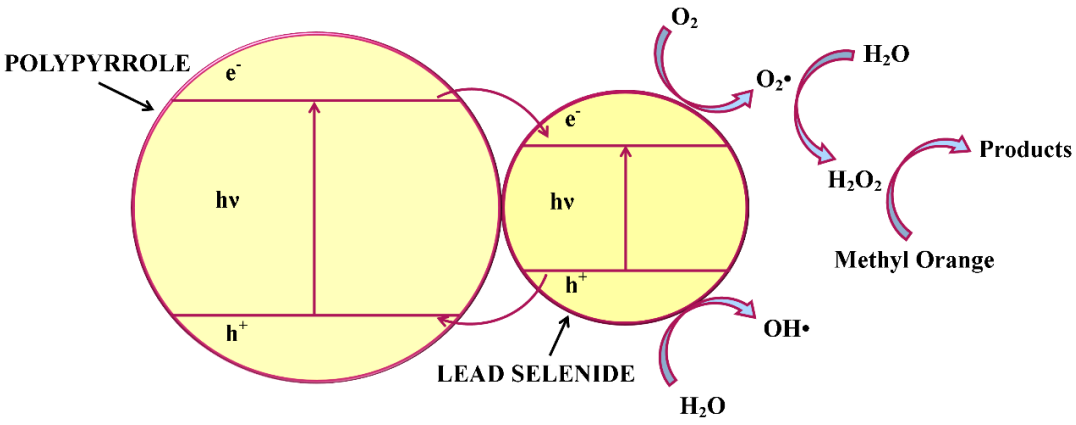

Fig. 6. Mechanism of methyl orange degradation

Effect of Irradiation Time

In order to detect the potential for degradation of ppy/lead selenide nanocomposite on degradation of methyl orange the effect of irradiation time was studied at time intervals of 10 mins for 1 hour under 10 ppm concentration of methyl orange. The graph of degradation percentage was plotted against time as shown (Fig. 7) and the highest degradation was achieved at 30 mins at 17.52 %. The following experiments were conducted at the irradiation time of 30 mins.

Effect of Dose

The dose effect on the degradation potential of methyl orange dye is examined by increasing the dose by 2 mg until the degradation is the highest. Dose 32 mg resulted in the highest degradation. The percentage graph of degradation was compared with dose (Fig. 8). The percentage degradation for ppy/lead selenide increased from 17.52% to 48.28%. The rise in the active site, which releases the radical •OH and O2• is a consequence. But the rise in the catalyst also decreased light transmission after some doses [20]. The rest of the parameters were studied at irradiation time of30 mins with the dose of 32 mg.

Effect of Concentration

The concentration effect was first analyzed at concentrations of 10 ppm, 20 ppm, 30 ppm and 40 ppm where the highest degradation was observed by 10 ppm. The effect was then examined for 2 ppm, 4 ppm, 6 ppm and 8 ppm concentration. The highest degradation was observed at 2 ppm, where the value for ppy/lead selenide nanocomposite was 65.06 % (Fig. 9). The initial dye concentration is a factor that influences the dye's adsorption. The increased dye concentration increases the amount of the dye molecule on the photocatalyst's surface adsorbed. This leads to fewer photons reaching the photocatalyst surface which reduces the output of radicals •OH and O_2• [20].

Effect of pH

The pH impact analysis was carried out using the optimized radiation time, dose and concentration condition for 2, 4, 6, 8 and 10. The highest percentage of degradation at pH 6 was 83.13%. the graph of change in pH was plotted against the degradation percentage (Fig. 10).The primary oxidation species with the acidic pH are the positive holes (h+).The formation of H_2O_2 by reaction of electron with O_2 and H_2O and H_2O_2 in the case of higher acidic degradation rates, which can therefore be taken into account in the ppy/lead selenide nanocomposite as the degradation at a slightly acidic pH was the highest[19,21].

Comparison of The Different Parameters

A box plot was plotted to compare the effects of the different parameters for ppy/lead selenide nanocomposite (Fig. 11). The box plot indicated that the change in the concentration has the highest impact and change in irradiation time had the least. We can understand that various parameters influence the degradation of methyl orange in a different manner and the change in concentration has the highest effect.

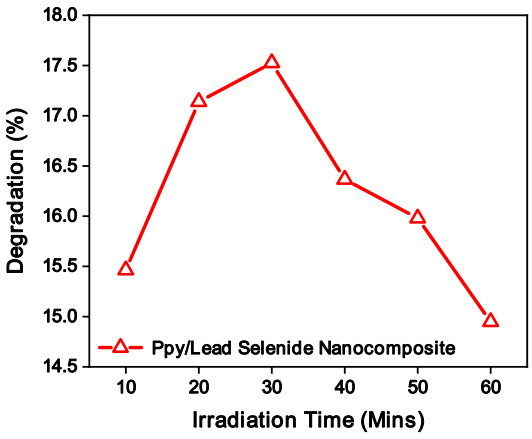

Fig. 7. Effect of irradiation time for ppy/ lead selenide nanocomposite

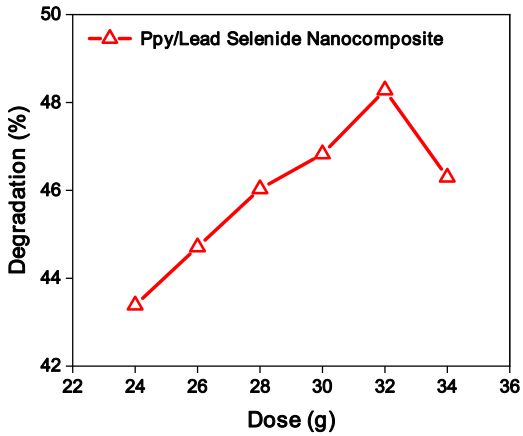

Fig. 8. Effect of dose for ppy/ leadselenide nanocomposite

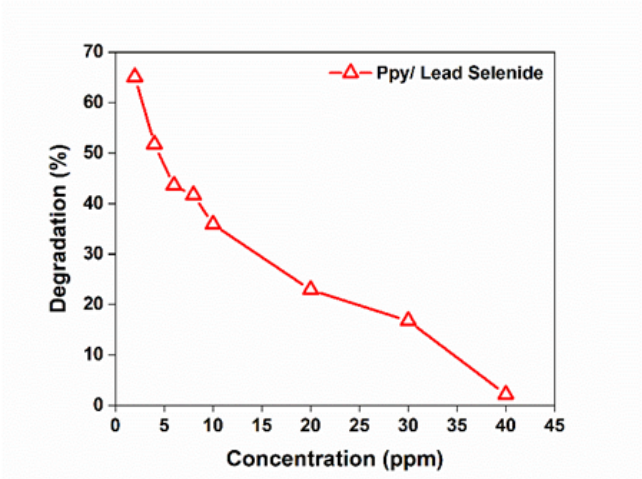

Fig. 9. Effect of concentration for ppy/ lead selenide nanocomposite

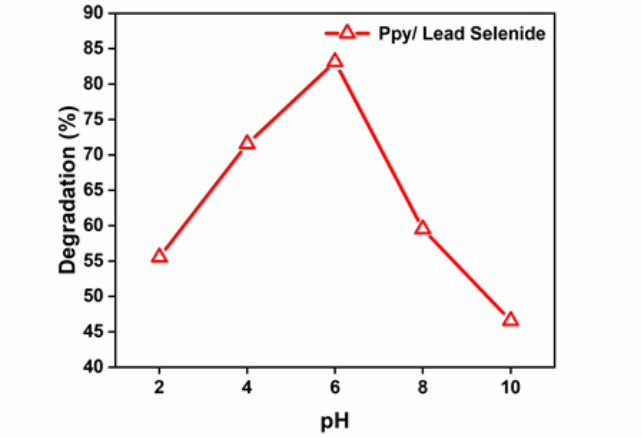

Fig. 10. Effect of pH for ppy/ lead selenide nanocomposite

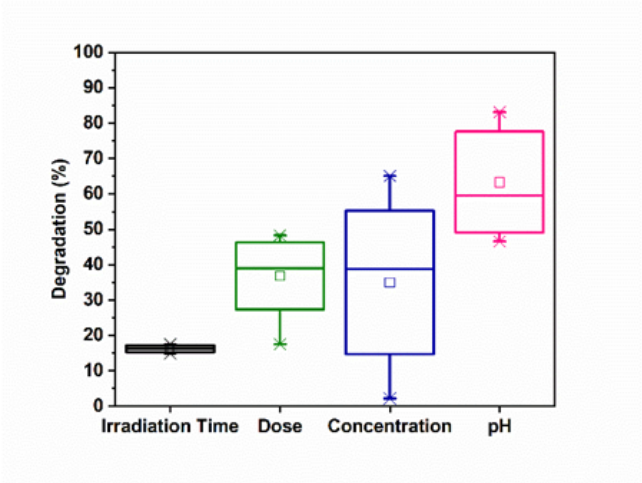

Fig. 11. Comparison of effect of different parameters of ppy/ lead selenide nanocomposite

Isotherms

The Freundlich, Langmuir and Temkin isotherm models were tested for the study [22–24].

Freundlich isotherm model takes into account the heterogeneity of the surface, the active site distribution and its energy and the logarithmic changes in enthalpy. The Freundlich equation is

$$q_e = K_F C_e^{1/n} \qquad (v)$$

Where q_e is the amount of dye degraded per unit mass of nanomaterials (mg/g), C_e is equilibrium concentration (mg/L), K_F and n are Freundlich equilibrium constants

The Langmuir Isotherm model has been frequently used and often used in processes of degradation and adsorption. Langmuir isotherm supposes that the uniform monolayer adsorption of dyes takes place on adsorbent surface.A 0 to 1 separation factor shows the surface adsorption process of dyes on the composite. The Langmuir equation is

$$qe = \frac{qm\ KLCe}{1+KL\ Ce} \qquad (vi)$$

Where C_e, equilibrium concentration, q_m and K_L are the Langmuir constants related to maximum degradation capacity (mg/g), and the relative energy of degradation (L/mg), respectively.

An equilibrium parameter RL (also known as the separation factor), which is dimensionless and constant, is able to articulate the critical features of the Langmuir isatherm.

$$R_L = \frac{1}{1+KL\ Co} \qquad (vii)$$

Where, C_o is initial concentration and K_L is the constant related to the energy of adsorption. The value of R_L indicates the adsorption nature to be linear if R_L =1, unfavorable if R_L> 1, favorable if 0 < R_L<1 and irreversible if R_L = 0.

The Temkin isotherm model takes into account the adsorbent-adsorbent interaction and assumes that the adsorption heat of all molecules is reduced linearly instead of logarithmic with coverage without very low and large values. The Temkin equation is

$$q_e = B \ln A_T + B \ln C_e \qquad (viii)$$

Where B is the Constant related to heat of sorption (J/mol) and A_T is the Temkin isotherm equilibrium binding constant (L/g).

For Freundlich isotherm, a graph of log Ce was plotted against log qe (Fig. 12), for Langmuir isotherm, Ce/qe against Ce (Fig. 12) and for Temkin isotherm, qe against ln Ce (Fig. 13). The isotherm data is also given in the Table. 2.

Freundlich isotherm correlation coefficient (R^2) for ppy/lead selenide nanocomposite was calculated to be 0.964. The values of n and $K_f$were calculated are -2.425(L/mg) and 1.694 (mg/g) respectively where the inverse of n denotes the adsorption of dye, a function of the adsorption strength and K_f, the adsorbent capacity for the adsorbate.

Langmuir isotherm correlation coefficient (R^2) was calculated to be 0.989. The q_m value and K_L were calculated are -8.340 (mg/g) and -0.171 (L/mg) respectively, where q_m, maximum monolayer coverage and K_L, constant related to the energy of the adsorption. the calculated value of RL was 0.997.

Temkin Isotherm correlation coefficient (R^2) was0.981. The A_T value and the B value were 0.151 (L/g) and -0.884 (J/mol) respectively where A_T, Temkin isotherm equilibrium binding constant and B, constant related to the heat of sorption.

The value of n was calculated to be less than 1 which shows adsorption was unfavourable. The value calculated for RL indicated a linear and favourable adsorption, since RL value was greater than 0 but less than 1. The adsorption process was also endothermic because of the negative value of B. In the Langmuir isotherm model, the correlation coefficient (R^2) of the study shows that the value is nearest to 1 which is indicative that as compared to Freundlich and Temkin isotherm models, the Langmuir isotherm model represents the adsorption process better. [25,26].

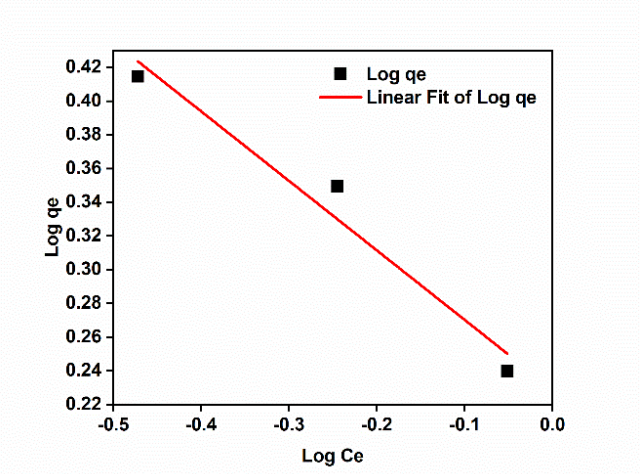

Fig. 12. Freundlich isotherm ppy/ lead selenide nanocomposite

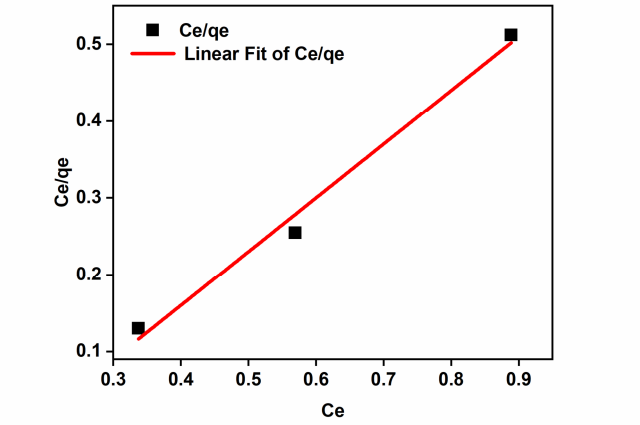

Fig. 13. Langmuir Isotherm of ppy/ lead selenide nanocomposite

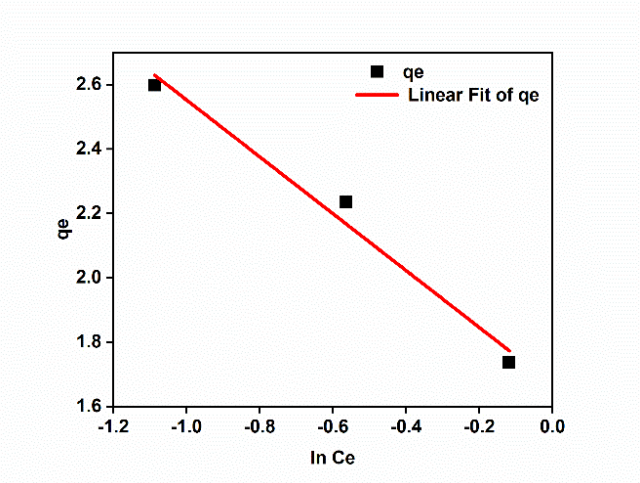

Fig. 14. Temkin Isotherm of ppy/ lead selenide nanocomposite

Table. 2. Isotherm constants

Freundlich	K_f	n	R^2
	1.694	-2.425	0.964
Langmuir	K_L	q_m	R^2
	-0.171	-8.340	0.989
Temkin	A_T	B	R^2
	0.151	-0.884	0.981

Gas Sensing Analysis

The study is performed on a 10 x 10 cm x 10 cm x 10 cm chamber.In the gas chamber containing the ppy/lead nanocomposite gas sensor, concentrations of 2 ppm, 4 ppm, 6 ppm, 8 ppm and 10 ppm of ammonia were introduced. The diagrammatic representation of the ammonia gas sensing has been given below (Fig. 15).

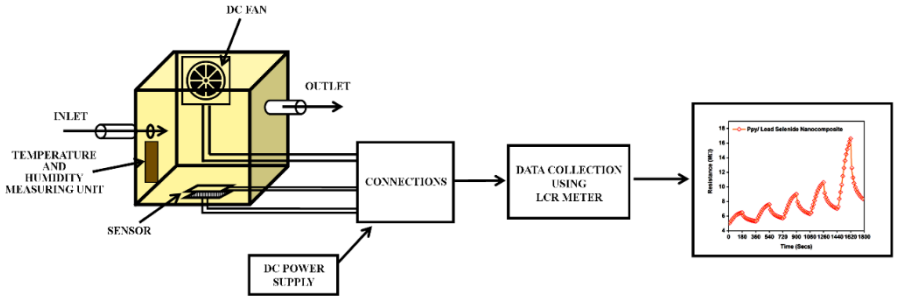

Fig. 15. Graphical diagram of the ammonia gas sensing

The introduction of ammonia gas causes the sensor to be saturated. The sensor was heated to 60°C to recover the sensor. During the analysis, the sensor was not completely retrieved due to the residual ammonia at the surface of the polymer chain in the sensor. Recovery decreases gradually with each exposure to ammonia (Fig. 16). The nanocomposite ppy/lead sensor has 23% sensitivity of 2 ppm, 30.32% of 4 ppm, 36.42% of 6 ppm, 40.64% of 8 ppm and 57.78% of 10 ppm of the ammonia gas sensor (Fig. 17). With rising ammonia concentration, the sensitivity of the sensor increases.

The study focuses on the use of ppy/ lead selenide nanocomposite as material dual applicability. In the study, photocatalytic behavior and ammonia gas sensitivity were explored. Response time, recovery time and selectivity of the sensor are areas which are left open for further sensor optimization study.

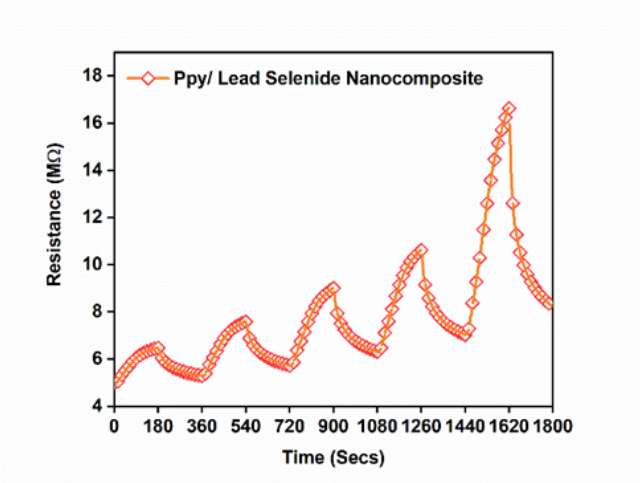

Fig. 16. Resistance vs Time graph of ppy/lead selenide nanocomposite

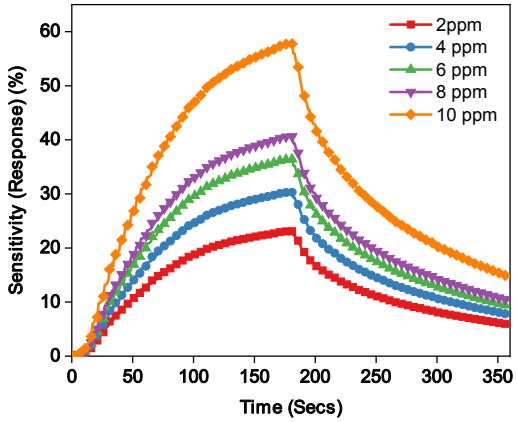

Fig. 17. Sensitivity (Response) vs Time graph of ppy/lead selenide nanocomposite

In the study, lead selenide nanomaterials were synthesized using co-precipitation method and polymerization ofpyrrolewas done in the presence of the synthesized lead selenide nanomaterial to prepare ppy/lead selenide nanocomposite. The synthesized ppy/lead selenide nanocomposite was able to degrade methyl orange upto 83.13 % under optimized condition of Irradiation time with UV light, dose of nanomaterial, concentration of dye and pH of the dye solution. The final optimized conditions were irradiation time - 30 mins, dose - 32 mg for ppy/lead selenide nanocomposite, concentration – 2 ppm concentration of methyl orange and pH – 6 for ppy/lead selenide nanocomposite. The sensor made from ppy/lead selenide nanocomposite has a sensitivity of 57.78 % at 10 ppm of ammonia gas. The study indicated that the photocatalytic potential of ppy/lead selenide nanocomposite is viable material for degradation of methyl orange and ammonia gas sensing.

REFERENCES

1. Sharma, H.K., &Sharma, M.V (2018). Nanomaterials: Sources, Applications and Toxicity. Journal of Nanoscience Nanoengineering and Applications 8:33–35
2. Sharma, H.K., Pandey, G., Shrivastava, S., Tomar, V (2010).Nanosilver Synthesis Under Control of Ligands Containing Azoresorcinol Group by Laser Irradiation. Nanoscience and Nanotechnology Letters 2:58–61
3. Pandey, G., Shrivastav, S., Sharma, H.K (2014). Role of solution pH and SDS on shape evolution of PbS hexagonal disk and star/flower shaped nanocrystals in aqueous media. Physica E: Low-dimensional Systems and Nanostructures 56:386–392
4. Pandey, G., Sharma, H.K., Srivastava, S.K., Kotnala, R.K (2011). γ-MnS nano and micro architectures: synthesis, characterization and optical properties. Materials Research Bulletin 46:1804–1810
5. Pandey, G., & Sharma, H.K (2010). A new approach of synthesis of micro/nanoscale HgS spheres. Synthesis and Reactivity in Inorganic, Metal-Organic, and Nano-Metal Chemistry 40:312–318

6. Bakueva, L., Musikhin, S., Hines, M. A., Chang, T. W., Tzolov, M., Scholes, G. D., & Sargent, E. H (2003). Size-tunable infrared (1000–1600 nm) electroluminescence from PbS quantum-dot nanocrystals in a semiconducting polymer. Applied physics letters, 82(17): 2895-2897. https://doi.org/10.1063/1.1570940
7. Andries, A., Bivol, V., Prisacar, A., Sergheev, S., Meshalkin, A., Robua, S., Barbaa, N. and Sirbub, N. (2005). Laser and electron induced structuring of thin films on the base of carbazolyl-containing polymers and polymer-ChNS compositions. Journal of Optoelectronics and Advanced Materials, 7(3), 1169-1178.
8. Tiwari, D.C., Atri, P., Sharma, R (2015). Sensitive detection of ammonia by reduced graphene oxide/polypyrrole nanocomposites. Synthetic Metals 203:228–234. https://doi.org/10.1016/ j.synthmet.2015.02.026
9. Iovu, M. S., Andries, A. M., Buzurniuc, S. A., Verlan, V. I., Colomeico, E. P., &Robu, S. V. (2006). New As2S3: Pr3*-polymer composite materials. Journal of optoelectronics and advanced materials, 8(1): 257-260.
10. PubChem Methyl orange. https://pubchem.ncbi.nlm.nih.gov/compound/23673835. Accessed 15 Dec 2020
11. Joshi, A., Gangal, S.A., Gupta, S.K (2011). Ammonia sensing properties of polypyrrole thin films at room temperature. Sensors and Actuators B: Chemical 156:938–942. https://doi.org/ 10.1016/j.snb.2011.03.009
12. Canada E &CC (2004). Common air pollutants: ammonia, Aem. https://www.canada.ca/en/ environment-climate-change/services/air-pollution/pollutants/common-contaminants/ammonia.html. Accessed 26 Mar 2020
13. Srivastava, P.,& Singh, K (2012). Synthesis of CdSe Nanoparticles By Solvothermal Route: Structural, Optical And Spectroscopic Properties. AML 3:340–344. https://doi.org/10.5185/amlett.2012.5341
14. Chitte, H.K., Shinde, G.N., Bhat, N.V., Walunj, V.E (2011). Synthesis of Polypyrrole Using Ferric Chloride (FeCl₃) as Oxidant Together with Some Dopants for Use in Gas Sensors. JST 01:47–56. https://doi.org/10.4236/jst.2011.12007
15. Arafat, M.M., Dinan, B., Akbar, S.A., Haseeb, A (2012). Gas sensors based on one dimensional nanostructured metal-oxides: a review. Sensors 12:7207–7258
16. Holzwarth, U., &Gibson, N. (2011). The Scherrer equation versus the'Debye-Scherrer equation'. Nature nanotechnology 6:534
17. Kumar, M., Mehta, A., Mishra, A., Singh, J., Rawat, M., &Basu, S. (2018). Biosynthesis of tin oxide nanoparticles using Psidium Guajava leave extract for photocatalytic dye degradation under sunlight. Materials Letters, 215: 121-124. https://doi.org/10.1016/j.matlet.2017.12.074
18. Hunge, Y. M., Yadav, A. A., &Mathe, V. L. (2018). Ultrasound assisted synthesis of WO3-ZnO nanocomposites for brilliant blue dye degradation. Ultrasonics sonochemistry, 45: 116-122. https://doi.org/10.1016/j.ultsonch.2018.02.052
19. Viswanathan, B. (2018). Photocatalytic degradation of dyes: An overview. Current Catalysis, 7(2), 99-121.
20. Kumar, A., & Pandey, G. (2017). A review on the factors affecting the photocatalytic degradation of hazardous materials. Mater. Sci. Eng. Int. J, 1(3): 1-10.
21. Muruganandham, M., & Swaminathan, M. (2004). Photochemical oxidation of reactive azo dye with UV–H2O2 process. Dyes and pigments, 62(3), 269-275.
22. Singh, R., Kulkarni, K., & Kulkarni, A. D. (2011). Application of appopolite in adsorption of heavy metals (Co and Ni) from waste water. Chem. Mater. Res, 1(2), 16-21.
23. Dubey, L., Sharma, H. K., &Khare, R. K. (2017). Removal of Zinc and Lead from Aqueous Solution using Low Cost Bioadsorbent Pennisetumglaucum (Bajara) Husk. Advances in Bioresearch, 8(4).
24. Dada, A. O., Olalekan, A. P., Olatunya, A. M., & Dada, O. J. I. J. C. (2012). Langmuir, Freundlich, Temkin and Dubinin–Radushkevich isotherms studies of equilibrium sorption of Zn2+ unto phosphoric acid modified rice husk. IOSR Journal of Applied Chemistry, 3(1): 38-45.
25. Igwe, J. C., &Abia, A. A. (2007). Adsorption isotherm studies of Cd (II), Pb (II) and Zn (II) ions bioremediation from aqueous solution using unmodified and EDTA-modified maize cob. EcléticaQuímica, 32(1): 33-42.
26. Edet, U.A., Ifelebuegu, A.O (2020). Kinetics, Isotherms, and Thermodynamic Modeling of the Adsorption of Phosphates from Model Wastewater Using Recycled Brick Waste. Processes 8:665